Journal of Hazardous Materials 393 (2020) 122348

Contents lists available at ScienceDirect

Journal of Hazardous Materials

journal homepage: www.elsevier.com/locate/jhazmat

Multiplex SERS-based lateral flow immunosensor for the detection of major mycotoxins in maize utilizing dual Raman labels and triple test lines

Wanjun Zhang[a,1], Shusheng Tang[b,1], Yongpeng Jin[a,1], Chunjiang Yang[c], Lidong He[d], Jiayi Wang[a], Yiqiang Chen[a,*]

[a] State Key Laboratory of Animal Nutrition, College of Animal Science and Technology, China Agricultural University, Beijing, 100193, China
[b] College of Veterinary Medicine, China Agricultural University, Beijing, China
[c] Ring Biotechnology Co Ltd, Bodaxing Industry Park, Beijing, 101111, China
[d] Department of Chemistry and Biochemistry, Florida State University, Tallahassee, FL, 32306, USA

GRAPHICAL ABSTRACT

Illustration of multiplex SERS-based lateral flow immunosensor for mycotoxins.

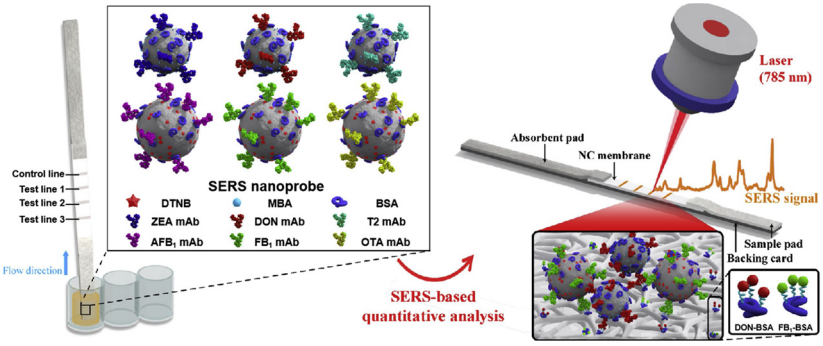

ARTICLE INFO

Editor: R. Teresa

Keywords:
Surface enhanced Raman scattering
Lateral flow
Immunoassay
Biosensor
Mycotoxin

ABSTRACT

A multiplex surface-enhanced Raman scattering (SERS)-based lateral flow immunosensor was developed to determine six major mycotoxins in maize. Two characteristic Raman reporter molecules—5,5-dithiobis-2-nitrobenzoic acid (DTNB) and 4-mercaptobenzoic acid (MBA)—were used to label the synthesized Au@Ag core-shell nanoparticles for the preparation of SERS nanoprobes as detection reagents. Six corresponding hapten-protein conjugates were prepared and dispensed on three test lines of nitrocellulose membrane with two conjugates on each line as capture antigens. This design facilitates the simultaneous detection of the six mycotoxins in a single test. After optimizing the experimental parameters of immunosensor, the limits of detection were as low as 0.96 pg/mL for aflatoxin B_1, 6.2 pg/mL for zearalenone, 0.26 ng/mL for fumonisin B_1, 0.11 ng/mL for deoxynivalenol, 15.7 pg/mL for ochratoxin A, and 8.6 pg/mL for T-2 toxin, respectively. The spiking experiment showed high accuracy with recovery of 78.9–106.2 % and satisfactory assay precision with the coefficient of variations below 16 %. Moreover, this assay can be completed in less than 20 min, and its detection results were consistent with that of liquid chromatography-mass spectrometry. Therefore, the developed SERS-based lateral flow immunosensor is a promising approach for mycotoxin detection in the field.

* Corresponding author.
E-mail address: yqchen@cau.edu.cn (Y. Chen).
[1] These authors contribute equally to this work.

https://doi.org/10.1016/j.jhazmat.2020.122348
Received 21 January 2020; Received in revised form 7 February 2020; Accepted 17 February 2020
Available online 19 February 2020

1. Introduction

Mycotoxins are toxic secondary metabolites produced by toxic fungi on contaminated crops during harvest, storage, and processing (Bennett and Klich, 2003; Brase et al., 2009). The common mycotoxins include aflatoxin B_1 (AFB_1), zearalenone (ZEA), fumonisin B_1 (FB_1), deoxynivalenol (DON), ochratoxin A (OTA), and T-2 toxin (T2). The intake of these mycotoxins can pose potential hazards to human and animal health such as carcinogenicity, immunotoxicity, neurotoxicity, nephrotoxicity, and estrogenic effects (Peraica et al., 1999; Wu et al., 2014). Consequently, maximum tolerable levels of major mycotoxins in agricultural products have been established by different countries and regions (Table S1). Moreover, recent studies have demonstrated that the contamination of mycotoxins with concentrations much lower than the maximum tolerable levels can also pose deleterious effects on animals (Alizadeh et al., 2015; Marin et al., 2016; Gaj et al., 2019). Therefore, the capability of detecting mycotoxins at low concentration is very important to protect the health of animals and humans.

Many analytical approaches including instrumental methods and bio-analytical methods have been developed to detect mycotoxins in diverse sample types (Shephard, 2016; DChauhan et al., 2016). Instrumental analyses mainly comprise liquid chromatography (LC) (Liu et al., 2019) and LC-tandem mass spectrometry (LC–MS/MS) (Santis et al., 2017; Romera et al., 2018; Sanches et al., 2019). These methods are often conducted in well-equipped laboratories and can produce accurate and precise analytical results, but they require expensive equipment, well-trained personnel, and sophisticated sample preparation with relative long turnaround time, which limits their use in the field. Because timely monitoring of mycotoxin contamination is very important in food and feed industry, various bio-analytical approaches such as enzyme immunoassay (Lai et al., 2017; Wang et al., 2018), lateral flow immunoassay (Urusov et al., 2016; Xu et al., 2019), and biosensors (Goud, 2018; Hossain and Maragos, 2018; Machado et al., 2018) have been developed (Table S2). These methods have the advantage of simplicity, rapidity, and low-cost, but most of them can only detect one or two mycotoxins in a single test. As mycotoxins generally co-contaminated in crops (Ibáñez-Vea et al., 2011; Smith et al., 2016), a method with higher multiplexing capability is in urgent need.

The surface-enhanced Raman scattering (SERS)-based lateral flow immunosensing assay is a novel analytical technology that combines SERS detection and lateral flow assay format (Wang et al., 2017). With the advantages of rapidity, high assay sensitivity, and multiplexing capability, it has the potential to be used for simultaneous detection of various low-level target analytes. In recent years, SERS-based lateral flow immunosensors have been developed for the detection of different target molecules such as interleukin-6 (Wang et al., 2019b), human chorionic gonadotropin (Tran et al., 2019), resistance protein A (Russo et al., 2019), and diclofenac (Deng et al., 2019). Moreover, several multiplex SERS-based lateral flow biosensors have been developed for the simultaneous measurement of respiratory viruses (Wang et al., 2019a) and cardiac biomarkers (Zhang et al., 2018) by setting two or three test lines on the detection zone of nitrocellulose membrane. However, these multiplexing formats did not fully take advantage of multiple-label SERS measurement. To further extend the multiplexing capability of SERS-based biosensing assay, we combined dual-Raman label and triple-line assay format to develop a multiplex SERS-based lateral flow immunosesnor for the simultaneous detection of six common mycotoxins in maize. To the best of our knowledge, this is the first rapid immunosensor with the multiplexing detection capability for six different types of target molecules. Moreover, the validation of this immunosensor was also demonstrated.

2. Materials and methods

2.1. Materials

Chemical standards of the six mycotoxins including AFB_1, ZEA, DON, FB_1, OTA, and T2, the Raman label molecules including 5′-dithiobis-2-nitrobenzoic acid (DTNB), *p*-mercaptobenzoic acid (MBA), *p*-aminothiophenol (PATP), *4*-mercaptophenylboronic acid (MPBA) bovine serum albumin (BSA), chloroauric acid, silver nitrate, trisodium citrate, Triton X-100, and Tween 20 were bought from Sigma-Aldrich (St. Louis, MO, USA). Goat anti-mouse second antibody was obtained from Jackson ImmunoResearch Inc. (West Grove, PA, USA). The nitrocellulose membrane CN 140 was purchased from Sartorius Stedim Biotech GmBH (Germany). The sample pad and absorbent pad were provided by Jieyi Biotechnology Co., Ltd. (Shanghai, China). The AFB_1-BSA, ZEA-BSA, DON-BSA, OTA-BSA, FB_1-BSA, and T2-BSA conjugates were synthesized in our lab (Supplementary material). The anti-AFB_1 monoclonal antibody (mAb), anti-ZEA mAb, and anti-T2 mAb were prepared by our group. The anti-DON mAb, anti-FB_1 mAb, and anti-OTA mAb were provided by Beijing NBGene Limited Company (Beijing, China). The HM 3030 Dispensing Platform and ZQ 2000 Guillotine Cutting Module were provided by ShangHai Kinbio Tech. Co. Ltd. (Shanghai, China).

2.2. Synthesis of gold nanoparticles (AuNPs) and Au@Ag core-shell nanoparticles (Au@Ag NPs)

The AuNPs with the size of 32 nm were first synthesized referring to the protocol of Frens (1973) with small modifications (Supplementary material). The Au@Ag NPs were then prepared (Blanco-Covián et al., 2017 as follows: Briefly, 20 mL of the synthesized AuNPs 32 nm were treated with 120 μL of 0.2 M ascorbic acid and 30 μL of 0.2 M silver nitrate and then reacted for 30 min under slow stirring. This process was considered to be a reaction cycle. After four or eighteen cycles, the resulting Au@Ag NPs 52 nm and 91 nm were centrifuged at 3,500 or 2,000 rpm for 20 min. The precipitate was re-suspended in 20 mL water and stored at 4 °C for use. The sizes of the synthesized AuNPs and Au@Ag NPs were then measured by transmission electron microscopy TEM, JEOL Inc., USA, and the core-shell structure of the selected Au@Ag NPs was further characterized by field emission transmission electron microscopy FETEM and X-ray energy dispersive spectroscopy EDS, Tecnai G2-F20, FEI, USA.

2.3. Preparation of the SERS nanoprobe

Briefly, the synthesized Au@Ag NPs (91 nm or 52 nm, 10 mL) were successively added with 0.1 M borate buffer (pH 8.5, 500 μL) and then with 1 mM DTNB (300 μL) for 91 nm Au@Ag NP or 1 mM MBA (100 μL) for 52 nm Au@Ag NP, respectively. After the incubation for 20 min at room temperature, 40 μL of 1.0 mg/mL anti-AFB_1 mAb, 30 μL of 1.0 mg/mL anti-FB_1 mAb, and 50 μL of 1.0 mg/mL anti-OTA mAb were separately added to the DTNB-Au@Ag NP complex solution; 20 μL of 1.25 mg/mL anti-ZEA mAb, 20 μL of 1.0 mg/mL anti-DON mAb, and 40 μL of 1.5 mg/mL anti-T2 mAb were separately added to the MBA-Au@Ag NP complex solution. The mixed solutions were incubated for 1 h with slight stirring. Finally, the mAb-DTNB-Au@Ag NP and mAb-MBA-Au@Ag NP conjugates were mixed with 2% BSA in borate buffer (2 mM, 1 mL) to block any unreacted sites on the surface of Au@Ag NPs. The solutions were centrifuged at 2000 or 3500 rpm for 20 min and the supernatant was removed. The precipitates were then repeatedly re-suspended and centrifuged for another time. Finally, the precipitates were re-suspended in 0.01 M phosphate buffer (pH 7.4, 10 mL) which was supplemented with BSA (0.2 %) and Triton X-100 (0.5 %). Finally, 20 μL of anti-AFB_1, 30 μL of anti-ZEA, 20 μL of anti-DON, 40 μL of anti-FB_1, 15 μL of anti-OTA, and 20 μL of anti-T2 SERS nanoprobes were added into the micro-plate well and freeze-dried for

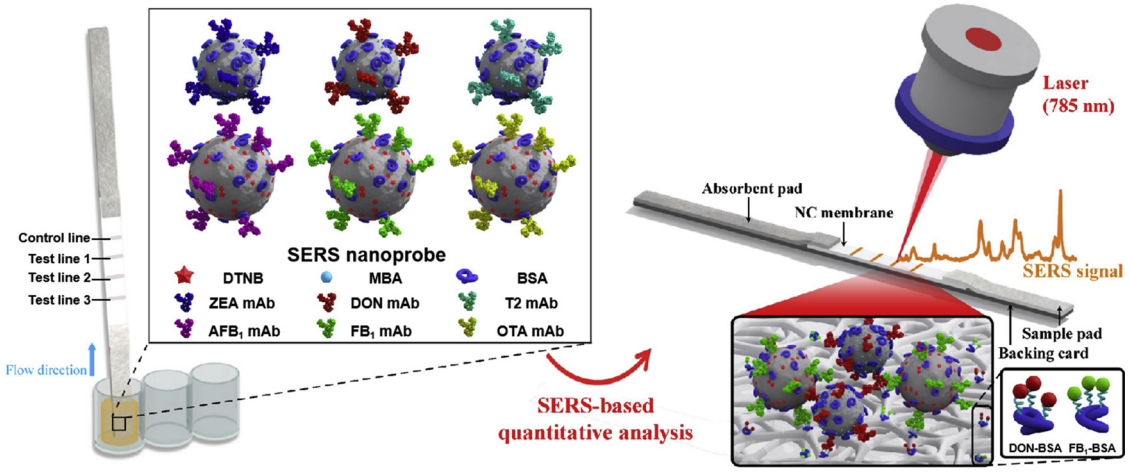

Fig. 1. Illustration of multiplex SERS-based lateral flow immunosensor for mycotoxins.

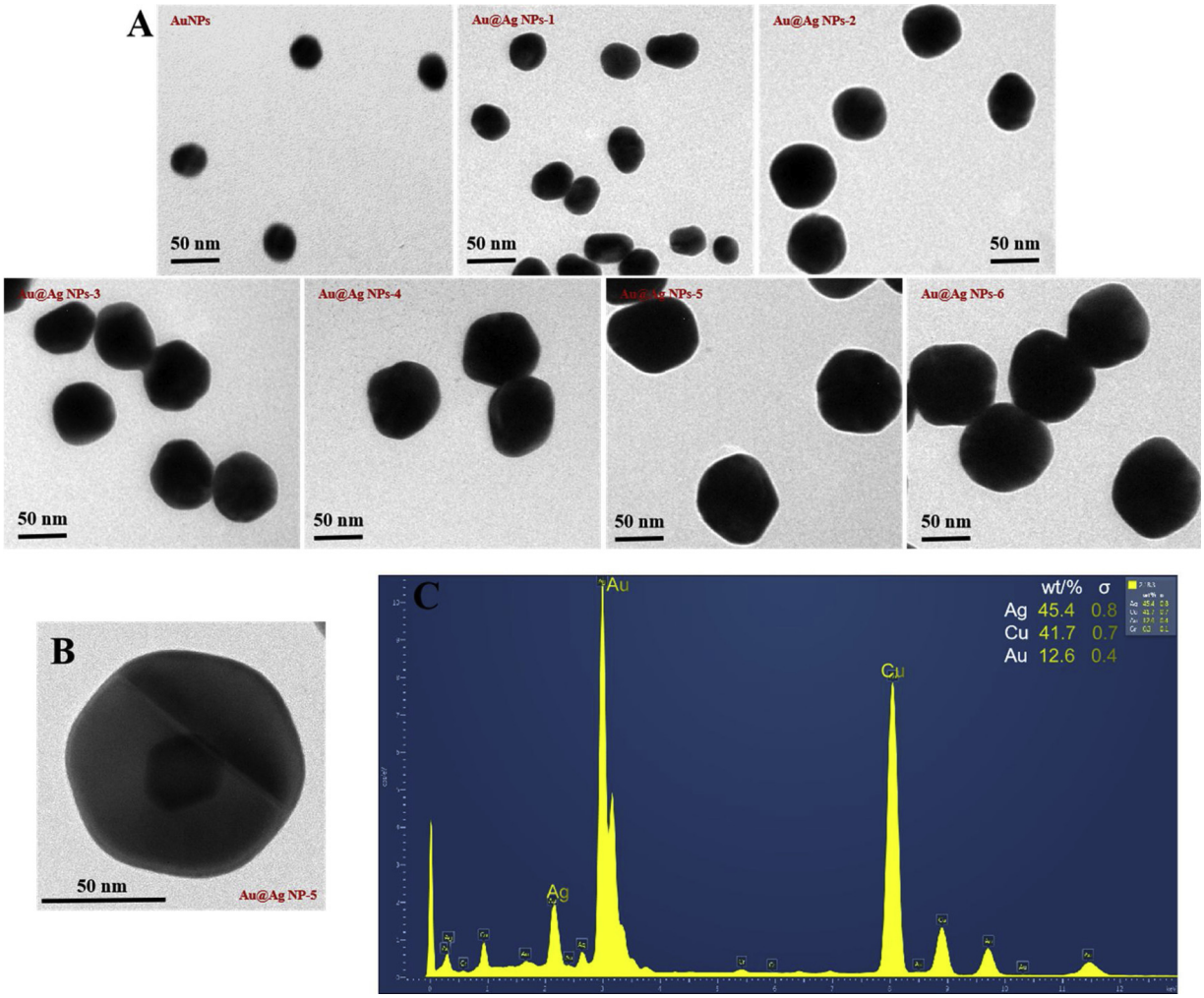

Fig. 2. The TEM images (A) of the synthesized AuNPs and Au@Ag NPs, the FETEM image (B) of typical Au@Ag NP, and the element mapping image (C) of EDS on Au@Ag NP. The sizes of the AuNPs and the six Au@AgNPs were measured by TEM to be 32 ± 3, 41 ± 4, 52 ± 6, 61 ± 7, 76 ± 9, 91 ± 11 and 99 ± 13 nm (n = 30), respectively.

use.

2.4. Assembly of the lateral flow strip

The six mycotoxin antigens and second antibody were dissolved in 0.05 M carbonate buffer (pH 9.5) and then immobilized onto the nitrocellulose membrane as capture antigens and capture antibody. Firstly, the AFB_1-BSA (0.2 mg/mL) and ZEA-BSA (0.15 mg/mL) conjugates were equally mixed. The OTA-BSA (0.2 mg/mL) and T2-BSA (0.1 mg/mL) conjugates were also equally mixed. The FB_1-BSA

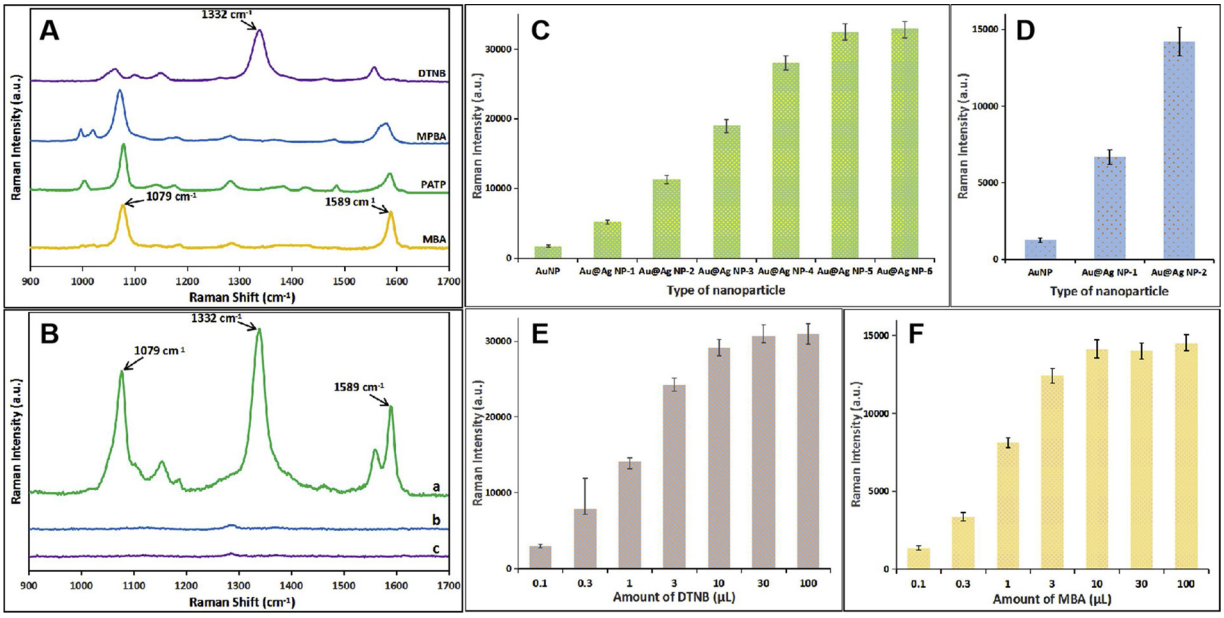

Fig. 3. The Raman spectra (A) of DTNB, MPBA, PATP, and MBA on Au@Ag NPs; the Raman spectra (B) of the mixture of DTNB/MBA-Au@Ag NP (a), the mixture of free DTNB and MBA (b), and Au@Ag NPs (c); the effect of nanoparticle size on the SERS intensity of DTNB-Au@Ag NP (C); the effect of nanoparticle size on the SERS intensity of MBA-Au@Ag NP (D), the effect of DTNB amount on SERS intensity (E), and the effect of MBA amount on SERS intensity (F).

(0.15 mg/mL) and DON-BSA (0.3 mg/mL) conjugates were equally mixed as well. The three combinations of antigens were then dispensed onto the three test lines of nitrocellulose membrane. Then, the goat anti-mouse second antibody (0.2 mg/mL) was applied to the control line of the nitrocellulose membrane (Fig. 1). The application volume was 1 μL/cm. Finally, the nitrocellulose membrane was put into a drying cabinet (37 °C) for 5 h, and it was kept in dry conditions until use.

To assemble the lateral flow strip (Fig. 1), the nitrocellulose membrane immobilized with capture antigen and second antibody was fixed on the center of an adhesive-backed card. Then the sample pad was secured on one side of the backing card with 2 mm overlapping with the nitrocellulose membrane. The other side of the backing card was pasted with absorbent pad which also slightly covered the nitrocellulose membrane for 2 mm. Finally, the assembled card was cut to the lateral flow strips with 4 mm-width and ready for use.

2.5. SERS assay procedure

The multiplex SERS-based immunosensing assay was performed as follows (Fig. 1). Briefly, the sample solution (200 μL) was mixed with the lyophilized SERS nanoprobe in the micro-plate well and incubated at room temperature for 2 min. Then the lateral flow strip was submerged into the micro-plate well, and the solution would flow up to the absorbent pad. After 10 min, the lateral flow strip was removed from the micro-well, and the immune-reaction was terminated. The SERS spectra from the test lines and the control line were acquired by a portable i-Raman® Plus Raman System. It was equipped with an excitation laser (785 nm), a microscope sampling system, and a charge-coupled device detector (B&W TEK, Newark, USA). The Raman spectra were collected from 175 to 3200 cm^{-1} with a spectral resolution of 4.5 cm^{-1}. The laser power was set at 60 mW. The integration time was set at 2000 ms for signal collection. All the Raman signals were treated by BWSpec Operation Software including smoothing and baseline correction.

2.6. Sample analysis

Four grams of the minced maize sample were weighed and then mixed with 40 mL of methanol-water (7:3, v/v). After votexing for 5 min, the extracted solution was centrifuged at 4,000 rpm for 10 min. Then, the supernatant was 10 times diluted with phosphate buffer saline (0.01 M, pH 7.4) and added with Tween 20 to a final concentration of 0.5 % (v/v). Finally, 200 μL of the mixed solution was subjected to the SERS-based immunosensor. For spiking experiments, blank maize samples without detectable mycotoxins were added with a series concentrations of the six mycotoxin solution. Then the spiked samples were treated and analyzed as described above.

3. Results and discussion

3.1. Scheme of the multiplex SERS-based lateral flow immunosensor

Fig. 1 shows the analytical principle of the developed immunosensor. Three combinations of capture antigens: AFB_1-BSA and ZEA-BSA, DON-BSA and FB_1-BSA, and OTA-BSA and T2-BSA, were correspondingly coated onto the three test lines of a nitrocellulose membrane. The detection reagents contain two types of SERS nanoprobes: the DTNB-labeled nanoprobes and the MBA-labeled nanoprobes. The DTNB-labeled SERS nanoprobes include anti-AFB_1, anti-FB_1, and anti-OTA nanoprobes, while the MBA-labeled SERS nanoprobes include anti-ZEA, anti-DON, and anti-T2 nanoprobes. If the maize sample was free of the six mycotoxins, the SERS nanoprobes would recognize the corresponding capture antigens to form three visible test line and produce intensive Raman signals at both 1332 cm^{-1} and 1589 cm^{-1} under laser excitation. The two bands 1332 cm^{-1} and 1589 cm^{-1} can be assigned to the symmetric stretches of the nitro group of DTNB (Yang et al., 2014) and the aromatic ring of MBA (Guo et al., 2019), respectively. Nevertheless, if the sample contained one type of mycotoxins, the mycotoxin would bind with the corresponding SERS nanoprobe and hinder its interaction with the capture antigen. Thus, there were fewer SERS nanoprobes and less signal produced on the test line. If sufficient mycotoxin molecules were in the sample, they would completely prevent the SERS nanoprobes from recognizing the capture antigens. Thus, the corresponding SERS nanoprobes would not be captured on the test line, and consequently no characteristic Raman signal can be produced. Despite of negative or positive sample, the second antibody on the control line can always recognize the SERS nanoprobes, and strong

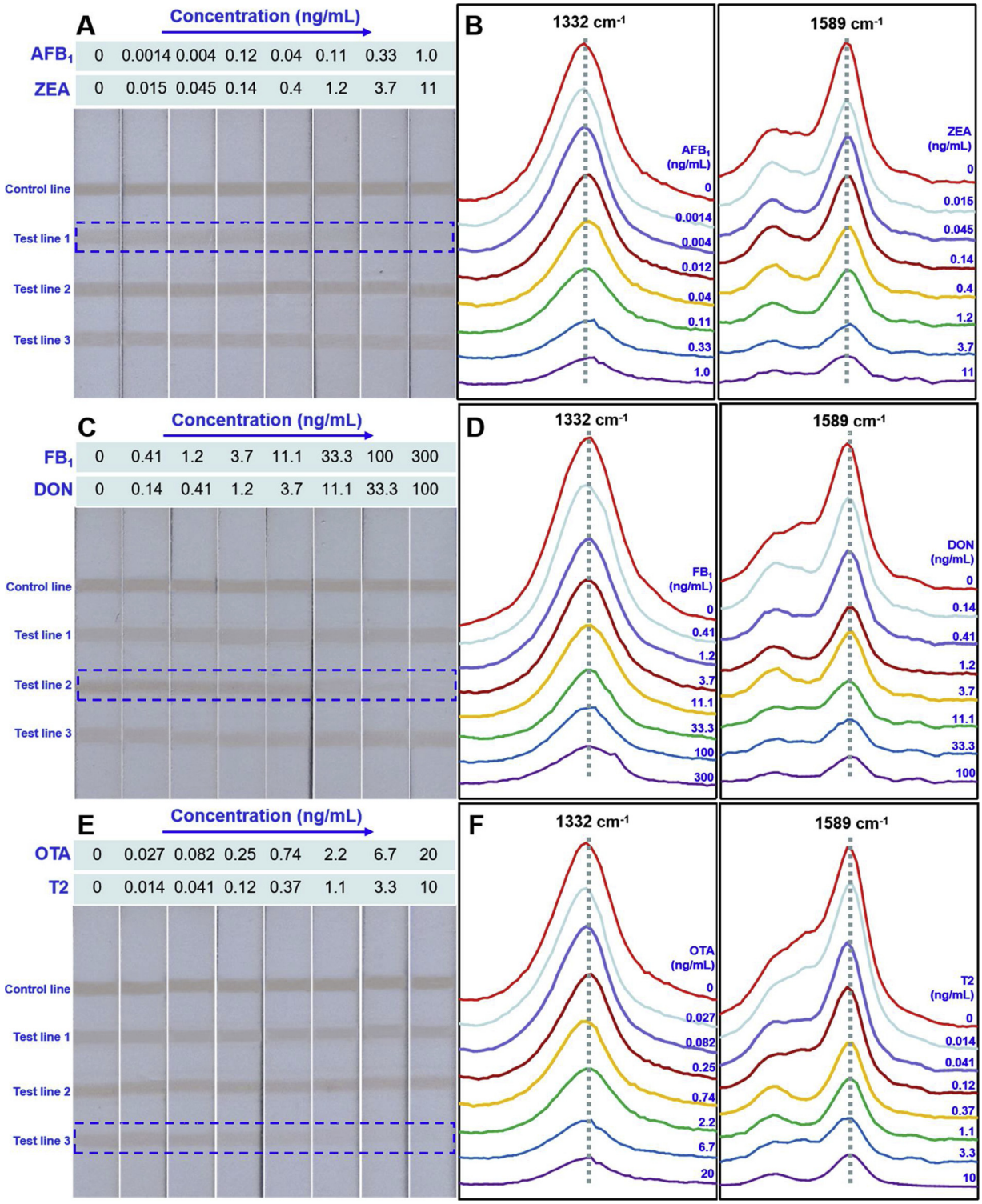

Fig. 4. Typical photo images of SERS-based lateral flow strips (A, C, E) and corresponding SERS spectra (B, D, F) for the detection of the six mycotoxins.

Raman signals can be produced at both 1332 cm^{-1} and 1589 cm^{-1}. Quantitative analysis was performed with six calibration curves. The calibration curves were generated with SERS intensity of the spiked samples over the intensity of blank samples (B/B_0) versus the logarithmic concentrations of the six mycotoxins. The SERS intensity from the unknown sample was then compared with the calibration curves to determine the analyte concentrations.

3.2. Antibody characterization

Six monoclonal antibodies (mAbs) were selected for the preparation of SERS nanoprobes. The isotypes of these mAbs were determined as IgG_{2a}, IgG_1, IgG_{2b}, IgG_{2a}, IgG_1 and IgG_{2a} for anti-AFB_1, anti-ZEA, anti-FB_1, anti-DON, anti-OTA, and anti-T2 mAbs, respectivley. The affinities of these antibodies were represented by the 50 % inhibition concentrations (IC_{50}) of corresponding mycotoxins. The IC_{50} values for anti-AFB_1, anti-ZEA, anti-FB_1, anti-DON, anti-OTA, and anti-T2 mAbs

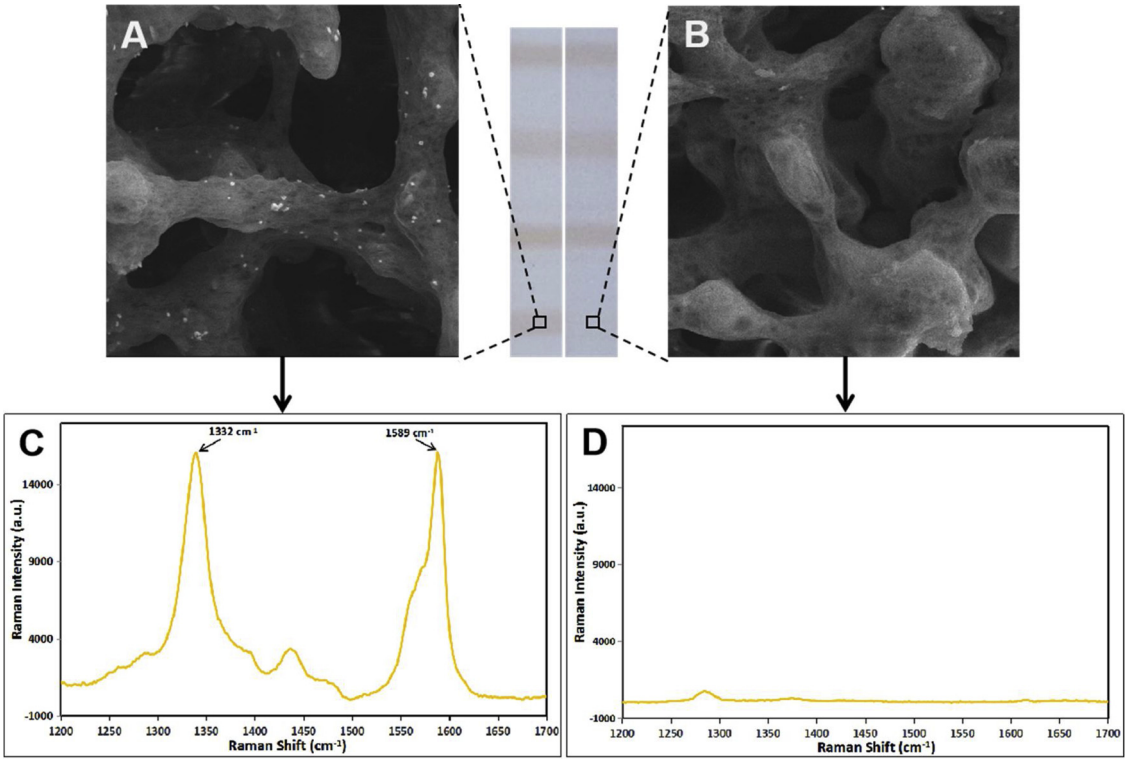

Fig. 5. Representative SEM images and Raman spectra from the test lines of negative sample (A, C) and strong positive sample (B, D).

Table 1
Spiked recoveries and coefficients of variation (CV) for mycotoxins in maize (n = 4).

Analyte	Spiked concentration (μg/kg)	Measured concentration (μg/kg)	Recovery (%)	CV (%)
AFB_1	1	1.062	106.2	9.9
	5	4.675	93.5	13.2
	10	8.87	88.7	12.7
	20	16.64	83.2	15.6
ZEA	5	4.865	97.3	15.2
	20	16.94	84.7	10.8
	60	52.92	88.2	13.9
	150	118.35	78.9	14.1
DON	50	52.25	104.5	10.3
	200	175.4	87.7	13.9
	1000	916	91.6	12.8
	2000	1622	81.1	14.4
FB_1	200	204.6	102.3	11.1
	400	366.8	91.7	9.3
	1000	849	84.9	11.7
	4000	3180	79.5	15.5
OTA	5	4.885	97.7	12.9
	10	8.84	88.4	9.3
	20	16.54	82.7	10.3
	100	84.6	84.6	13.7
T-2 toxin	5	5.025	100.5	11.9
	20	18.54	92.7	9.3
	40	32.52	81.3	14.2
	100	87.7	87.7	13.7

were measured to be 0.23, 1.2, 16.6, 20.3, 3.8 and 2.7 ng/mL, respectively, demonstrating that all the mAbs have strong affinities to corresponding mycotoxins (Table S3). The specificities of these antibodies were expressed as the cross-reactivity value which was calculated as follows: Cross-reactivity value = (IC_{50} value of analyte)/(IC_{50} value of interferents) × 100 %. The result indicated that the six mAbs can specifically recognize the corresponding types of mycotoxins and would not interact with other irrelevant mycotoxins. It should be noted that the mAb against AFB_1 can recognize its analogs including AFB_2, AFG_1 and AFG_2 with the cross-reactivities of 81 %, 66 % and 68 %, respectively. The mAb against FB_1 can simultaneously interact with its analog FB_2 with the cross-reactivity of 91 %, and the mAb against T-2 toxin can recognize HT-2 toxin with the cross-reactivity of 119 %. Thus, these three mAbs are class-specific antibodies and could be used for the detection of the corresponding mycotoxin subtypes. These results demonstrated that the six mAbs have strong affinities and high specificity, and hence they could be used for the development of a robust SERS-based lateral flow immunosensor.

3.3. Preparation and characterization of the SERS nanoprobe

Because Au@Ag NPs can produce stronger SERS enhancement than pure gold substrates (Blanco-Covián et al., 2017), we synthesized six different sizes of Au@Ag NPs by tuning the volume of silver-staining solution added. The TEM images showed that the sizes of the Au@Ag NPs were correspondingly increased from 32 to 99 nm (32 ± 3, 41 ± 4, 52 ± 6, 61 ± 7, 76 ± 9, 91 ± 11 and 99 ± 13 nm) with increasing silver-staining solution volume (Fig. 2A). The FETEM image further indicated that the Au@Ag NP comprises a core-shell structure (Fig. 2B), and the single-particle X-ray energy dispersive spectroscopy (EDS) indicated a high concentration of Ag (Fig. 2C). These data confirm that the Au@Ag NPs were successfully synthesized.

To prepare the SERS nanoprobe, a layer of Raman molecules was placed on the nanoparticle. The four common Raman labels including DTNB, PATP, MPBA, and MBA (Granger et al., 2016; Wang et al., 2017) were selected for labeling, and their corresponding SERS spectra were obtained. Fig. 3A shows that the characteristic bands of DTNB in the SERS spectrum primarily consisted of 1332, 1059, and 1558 cm^{-1}; the characteristic bands of PATP, MPBA, and MBA were at 1079 and 1589 cm^{-1}. The MBA, PATP, and MPBA molecules share major common characteristic bands, and the characteristic bands of DTNB with MBA, PATP, and MPBA are well resolved. As the PATP and MPBA labels were observed to lead to aggregation of Au@Ag NPs, the DTNB and MBA Raman labels were finally selected for duplex labeling during

the preparation of SERS nanoprobes. The most intense band of DTNB at 1332 cm^{-1} and the second-most intense band of MBA at 1589 cm^{-1} were used for quantitative analysis because these two bands have no overlap with each other. As a result, duplex detection of different target analytes on a single test line was achieved by labeling Au@Ag NPs with DTNA or MBA followed by coupling with different anti-mycotoxin antibodies.

The Raman intensities of DTNB/MBA-Au@Ag NP complexes and free DTNB/MBA at the identical Raman reporter concentration were compared to examine the SERS enhancement effect of the newly synthesized Au@Ag NPs. Fig. 3B shows the DTNB-Au@Ag NP and MBA-Au@Ag NP complexes generated strong SERS signal at 1332 cm^{-1} and 1589 cm^{-1}, respectively, while free DTNB and MBA at the same concentration did not generate a measurable signal. Moreover, it was observed that the Au@Ag NPs alone would not produce any SERS signal (Fig. 3B); and therefore these results demonstrated that the Raman intensity of DTNB and MBA was greatly enhanced by Au@Ag NPs when these Raman molecules were absorbed onto the surface of Au@Ag NP.

The effect of the Au@Ag NP size on SERS intensity was also evaluated. DTNB and MBA solution were added into the Au@Ag NP solutions to a saturated level. The generated DTNB/MBA-Au@Ag NP complexes were then subjected to SERS analysis. The results showed that with increased size of Au@Ag NP, the SERS intensity of both DTNB-Au@Ag NP and MBA-Au@Ag NP complexes was dramatically increased (Fig. 3C and D). For DTNB labeling, the SERS intensity reached a plateau when the size of Au@Ag NP was larger than 91 nm (Fig. 3C and D); for MBA labeling, but the Au@Ag NP with the size larger than 52 nm was not stable after MBA modification. Thus, Au@Ag NPs with sizes of 91 nm and 52 nm were separately used for DTNB and MBA labeling in subsequent experiments.

The amounts of DTNB/MBA used for labeling were then optimized. Because the SERS intensity plateaued at 30 μL of DTNB and 10 μL of MBA solutions (Fig. 3E and F), these amounts of DTNB or MBA were used per mL of Au@Ag NP solution for labeling. After labeling DTNB/MBA on Au@Ag NP, the antibodies can be conjugated onto the nanoparticles by electrostatic and hydrophobic interaction (Lan et al., 2017). The quantity of antibodies used for conjugation is expected to affect the number of antibody molecule attached on Au@Ag NP which further influences SERS-based immunoassay sensitivity (Tobita et al., 2004; Saha et al., 2014). Thus, the assay sensitivities produced by different amounts of antibodies were compared to optimize the antibody amount. As a result, optimal antibody amounts with the best sensitivities at similar SERS signal were 4.0 μg of anti-AFB_1 antibody, 2.5 μg of anti-ZEA mAb, 2.0 μg of anti-DON mAb, 3.0 μg of anti-FB_1 mAb, 5.0 μg of anti-OTA mAb, and 6.0 μg of anti-T2 mAb per mL of Au@Ag NP solution.

3.4. Multiplex SERS-based lateral flow immunosensor

Several research groups have reported duplex or triplex SERS-based lateral flow immunosensors for diverse target molecules. For example, Wang et al. developed a magnetic SERS strip for the simultaneous detection of respiratory viruses with two test lines (2019), and Zhang et al. developed a triplex SERS lateral flow assay for cardiac biomarkers (2018). However, these multiplex SERS-based immunoassays are mainly based on two test lines or three test lines. These designs did not fully take advantage of the multiplex labeling capability in SERS assays. In this study, we used DTNB and MBA as two different Raman labels for the SERS detection and set three test lines with two diverse capture antigens per line. This facilitated the simultaneous detection of six mycotoxins on a single test strip. This design thus further extended the multiplexing capability of SERS-based lateral flow immunosensor.

The typical photographs of the lateral flow strips and the corresponding SERS spectra are shown in Fig. 4. The SERS intensities of the two characteristic peaks from each test line decreased with increasing concentrations of corresponding mycotoxins. This trend is expected for a competitive immunoassay. The SEM images on the lateral flow strip indicated that there are many SERS nanoprobes on the test line for the negative sample (0 ng/mL), while there are no observable SERS nanoprobes bound on the test line of the nitrocellulose membrane for strong positive sample (Fig. 5). This further confirms that the spectral features were generated by the SERS nanoprobes.

The dose-response curve shown in Fig. S1 plots the intensity of 1332 cm^{-1} and 1589 cm^{-1}: the strongest feature in the DTNB and MBA spectrum against the logarithmic value of mycotoxin concentration (Qian and Bau, 2004). The results showed that the signal had a linear reduction with a logarithmic rise in analyte concentration. The linear assay ranges were set at 0.0014–0.33 ng/mL ng/mL for AFB_1, 0.015–3.7 ng/mL for ZEA, 0.41–100 ng/mL for FB_1, 0.14–33.3 ng/mL for DON, 0.027–6.7 ng/mL for OTA, and 0.014–3.3 ng/mL for T2; the R^2 values were over 0.99 demonstrating satisfactory linearities.

3.5. Method validation

A spiked recovery experiment was performed to further validate the developed immunosensor. LC–MS/MS analysis was conducted to confirm that a blank maize sample did not contain detectable mycotoxins (Santis et al., 2017). This blank sample was then spiked with the six mycotoxins and analyzed via the SERS-based immunosensor. The SERS intensities of 1332 cm^{-1} and 1589 cm^{-1} on the three test lines were measured and were then applied to the corresponding calibration curves to calculate the concentrations of mycotoxins in sample solution. The assay sensitivities of this immunosensor was represented by the limits of detection (LOD). They were defined as the concentrations of mycotoxin corresponding to the mean SERS intensity of the blank samples (n = 20) minus twice the standard deviation of the blank measurement (Dufek et al., 2010). The LOD values were then determined to be 0.96 pg/mL for AFB_1, 6.2 pg/mL for ZEA, 0.26 ng/mL for FB_1, 0.11 ng/mL for DON, 15.7 pg/mL for OTA, and 8.6 pg/mL for T2, respectively. These values all meet the low-level detection requirements at the tolerable limits set by different countries and regions (Table S1). As compared with ELISA method using the same antibodies, the assay sensitivities of the SERS-based immunosensor for most mycotoxins were improved for more than one magnitude (Table S2).

In previous studies, different immunoassay or biosensors have been developed for the detection of diverse mycotoxins with the LODs ranging from several pg/mL to ng/mL (Table S2). For example, Zhu et al. (2018) developed a dual-competitive lateral flow aptasensor for AFB_1 in food and feedstuffs with the LOD of 0.1 ng/mL. Li et al. (2020) developed an electrochemical aptasensor for AFB_1 in peanut with the LOD of 0.016 ng/mL, and Tang et al. (2020) developed a nanobody-mediated FRET-based immunosensor for OTA in agro-product with LOD of 5 pg/mL. These immunosensors demonstrated excellent sensitivities and specificities, but they mainly focus on the detection of single mycotoxin. For the multiplexing detection, Hossain et al. (2018) developed an iSPR biosensor assay for ZEA, DON and T2 with LODs of 0.75, 1.2 and 0.6 ng/mL, respectively. Pagkali et al. (2018) developed a label-free monolithically integrated optoelectronic biosensor for AFB_1, FB_1 and DON with the LODs of 0.8, 5.6 and 24 ng/mL, respectively. Compared to the above immunoassays and biosensors, the sensitivities of the SERS-based lateral flow immunosensing assay (LFIA) developed in this study are similar or superior (Goud, 2018; Table S2). Moreover, the developed immunosensor can simultaneously detect six mycotoxins in a single test. This markedly extends the multiplexing capability of the current immunoassay for mycotoxins. In addition, the assay sensitivities of this immunosensor were also superior to that of typical LC–MS/MS method (Table S2), which facilitates the elimination of matrix effect in the immunosensing assay simply by the dilution of sample solution.

The accuracy and precision of this SERS-based immunosensor were tested with spiked recovery experiments. The results indicated that the recoveries of the mycotoxins from maize sample ranged from 78.9 %–106.2 % at the spiked concentrations; the coefficients of variation

(CV) were less than 16 % (Table 1). These metrics demonstrate that this immunosensor has satisfactory assay accuracy and precision. The reproducibility of this SERS-based lateral flow immunosensor was examined by detecting different concentrations of mycotoxins spiked in bank sample solution, using three batches of SERS nanoprobe and test strips. The result indicated that the assay variations from the three batches of detection were below 16 % (Table S4), demonstrating that the reproducibility of this immunosensor including the preparation of SERS nanoprobe and test strips was acceptable. The selectivity of the developed immunosensor was further evaluated by spiking common mycotoxins into blank sample solution and followed by the SERS-based LFIA. The result showed the detection of individual mycotoxins would not be interfered by other common mycotoxins (Fig. S2). Thus, the developed SERS-based lateral flow immunosensor can be specifically used for the rapid detection of the six mycotoxins in maize sample. To further validate the developed analytical method, the mycotoxin concentration in five maize samples collected from local market were determined by the developed SERS-based lateral flow immunosensor and the LC–MS/MS method (Santis et al., 2017) (Table S5), respectively. Four of the five samples were measured to contain more than one mycotoxin, and sample 5 was found contaminated with aflatoxins, ZEA and DON exceeding the maximum tolerable levels set by the EU and China. Moreover, the detection values measured by the immunosensor were in good agreement with that of the LC–MS/MS analysis, and the variations of the detection values were less than 17 %. For sample 1, it was measured to contain 0.19 μg/kg of aflatoxins by the developed immunosensor, but this concentration was lower than the limit of detection of the LC–MS/MS analysis. On the other hand, all the negative results given by the developed immunosensor were also confirmed to be negative by the LC–MS/MS analysis, indicating that the immunosensor would not produce any false negative results. Therefore, these results demonstrated that the developed SERS-based lateral flow immunosensor can be used for actual sample analysis.

4. Conclusion

In this study, a novel multiplex SERS-based lateral flow immunosensor was successfully developed to simultaneously detect six major mycotoxins in maize. The LODs of this immunosensor are lower than instrumental analysis and most other biosensors, and they are all far below the tolerable limits set by the EU, USA and China. Moreover, this immunosensor demonstrated satisfactory assay accuracy, precision and specificity, and the detection time is less than 20 min. Thus, it can be utilized for the rapidly monitoring of the common mycotoxins in maize sample. Furthermore, the utilization of dual Raman labels and triple test lines greatly improves the multiplexing capability of the current immunoassay format. Therefore, we believe that this novel SERS-based lateral flow immunosensor holds great promise for further use in food safety supervision and biomedical diagnostics.

CRediT authorship contribution statement

Wanjun Zhang: Methodology, Investigation, Software. **Shusheng Tang:** Writing - original draft, Formal analysis, Visualization. **Yongpeng Jin:** Investigation, Validation, Data curation. **Chunjiang Yang:** Resources, Validation. **Lidong He:** Writing - original draft. **Jiayi Wang:** Visualization. **Yiqiang Chen:** Conceptualization, Writing - review & editing, Supervision, Funding acquisition.

Declaration of Competing Interest

The authors declare that they have no known competing financial interests or personal relationships that could have appeared to influence the work reported in this paper.

Acknowledgments

The authors would like to thank the financial support of Chinese Universities Scientific Fund (201810019112). We also would like to thank LetPub (www.letpub.com) for its linguistic assistance during the preparation of this manuscript.

Appendix A. Supplementary data

Supplementary material related to this article can be found, in the online version, at doi:https://doi.org/10.1016/j.jhazmat.2020.122348.

References

Alizadeh, A., Braber, S., Akbari, P., Garssen, J., Fink-gremmels, J., 2015. Deoxynivalenol impairs weight gain and affects markers of gut health after low-dose, short-term exposure of growing pigs. Toxins 7, 2071–2095.
Bennett, J.W., Klich, M., 2003. Mycotoxins. Clin. Microbiol. Rev. 16, 497–516.
Blanco-Covián, L., Montes-García, V., Girard, A., Fernández-Abedul, M.T., Pérez-Juste, J., Pastoriza-Santos, I., Faulds, K., Graham, D., Blanco-López, M.C., 2017. Au@Ag SERRS tags coupled to a lateral flow immunoassay for the sensitive detection of pneumolysin. Nanoscale 9, 2051–2058.
Brase, S., Encinas, A., Keck, J., Nising, C.F., 2009. Chemistry and biology of mycotoxins and related fungal metabolites. Chem. Rev. 109, 3903–3990.
DChauhan, R., Singh, J., Sachdev, T., Basu, T., Malhotra, B.D., 2016. Recent advances in mycotoxins detection. Biosens. Bioelectron. 81, 532–545.
Deng, D., Yang, H., Liu, C., Zhao, K., Li, J., Deng, A., 2019. Ultrasensitive detection of diclofenac in water samples by a novel surface- enhanced Raman scattering (SERS)-based immunochromatographic assay using Ag MBA@SiO_2-Ab as immunoprobe. Sens. Actuator B-Chem. 283, 563–570.
Dufek, E.J., Ehlert, B., Granger, M.C., Sandrock, T.M., Legge, S.L., Herrmann, M.G., Meikle, A.W., Porter, M.D., 2010. Competitive surface-enhanced Raman scattering assay for the 1,25-dihydroxy metabolite of vitamin D_3. Analyst 135, 2811–2817.
Frens, G., 1973. Controlled nucleation for the regulation of the particle size in monodisperse gold suspensions. Nat. Phys. Sci. 241, 20–22.
Gaj, M., Rykaczewska, A., 2019. Time-dependent changes in the intestinal microbiome of gilts exposed to low zearalenone doses. Toxins 11, 296–321.
Goud, K.Y., Kumar, S., Gobi, K.V., Kim, K., 2018. Progress on nanostructured electrochemical sensors and their recognition elements for detection of mycotoxins: a review. Biosens. Bioelectron. 121, 205–222.
Granger, J.H., Schlotter, N.E., Crawford, A.C., Porter, M.D., 2016. Prospects for point-of-care pathogen diagnostics using surface-enhanced Raman scattering (SERS). Chem. Soc. Rev. 45, 3865–3882.
Guo, J., Zhang, X.L., Li, P., Han, R., Liu, Y.W., Han, X.X., Zhao, B., 2019. Surface-enhanced Raman scattering (SERS) as a probe for detection of charge-transfer between TiO2 and CdS nanoparticles. New J. Chem. 43, 230–237.
Hossain, Z., Maragos, C.M., 2018. Gold nanoparticle-enhanced multiplexed imaging surface plasmon resonance (iSPR) detection of Fusarium mycotoxins in wheat. Biosens. Bioelectron. 101, 245–252.
Ibáñez-Vea, M., Martínez, R., González-Peñas, E., Lizarraga, E., López de Cerain, A., 2011. Co-occurrence of aflatoxins, ochratoxin A and zearalenone in breakfast cereals from Spanish market. Food Cont. 22, 1949–1955.
Lai, W., Wei, Q., Xu, M., Zhuang, J., Tang, D., 2017. Enzyme-controlled dissolution of MnO_2 nanoflakes with enzyme cascade amplification for colorimetric immunoassay. Biosens. Bioelectron. 89, 645–651.
Lan, L., Yao, Y., Ping, J., Ying, Y., 2017. Recent advances in nanomaterial-based biosensors for antibiotics detection. Biosens. Bioelectron. 91, 504–514.
Li, Y., Liu, D., Zhu, C., Shen, X., Liu, Y., You, T., 2020. Sensitivity programmable ratiometric electrochemical aptasensor based on signal engineering for the detection of aflatoxin B_1 in peanut. J. Hazard. Mater. 387, 122001–122008. https://doi.org/10.1016/j.jhazmat.2019.122001.
Liu, Y., Li, W., Ding, Z., Li, Q., Wang, X., Liu, J., Zhuo, S., Shao, R., Ling, Q., Zheng, T., Li, J., 2019. Three-dimensional ordered macroporous magnetic photonic crystal microspheres for enrichment and detection of mycotoxins (II): the application in liquid chromatography with fluorescence detector for mycotoxins. J. Chromatogr. A 1604 (460475), 1–8.
Machado, J.M.D., Soares, R.R.G., Chu, V., Conde, J.P., 2018. Multiplexed capillary microfluidic immunoassay with smartphone data acquisition for parallel mycotoxin detection. Biosens. Bioelectron. 99, 40–46.
Marin, D.E., Motiu, M., Pistol, G.C., Gras, M.A., Calin, L., Stancu, M., Taranu, I., 2016. Diet contaminated with ochratoxin A at the highest level allowed by EU. World Mycotoxin J. 9, 587–596.
Pagkali, V., Petrou, P.S., Makarona, E., Peters, J., Haasnoot, W., Jobst, G., Haasnoot, W., Jobst, G., Moser, I., Gajos, K., Budkowski, A., Economou, A., Misiakos, K., Raptis, I., Kakabakos, S.E., 2018. Simultaneous determination of aflatoxin B_1, fumonisin B_1 and deoxynivalenol in beer samples with a label-free monolithically integrated optoelectronic biosensor. J. Hazard. Mater. 359, 445–453.
Peraica, M., Radic, B., Lucic, A., Pavlovic, M., 1999. Toxic effects of mycotoxins in humans. Bull. World Health Organ. 77, 754–766.
Qian, S., Bau, H.H., 2004. Analysis of lateral flow biodetectors: competitive format. Anal. Biochem. 326, 211–224.

Romera, D., Mateo, E.M., Mateo-Castro, R., Gómez, J.V., GimenoAdelantado, J.V., Jimenez, M., 2018. Determination of multiple mycotoxins in feedstuffs by combined use of UPLC-MS/MS and UPLC-QTOF-MS. Food Chem. 267, 140–148.

Russo, L., Sánchez-Purrà, M., Rodriguez-Quijada, C., Leonardo, B.M., Puntes, V., Hamad-Schifferli, K., 2019. Detection of resistance protein A (MxA) in paper-based immunoassays with surface enhanced Raman spectroscopy with AuAg nanoshells. Nanoscale 11, 10819–10827.

Saha, B., Evers, T.H., Prins, M.W.J., 2014. How antibody surface coverage on nanoparticles determines the activity and kinetics of antigen capturing for biosensing. Anal. Chem. 86, 8158–8166.

Sanches, A., Brites, C., Vila, A., Barbosa, J., Freitas, A., 2019. UHPLC-ToF-MS method for determination of multi-mycotoxins in maize: development and validation. Curr. Res. Food Sci. 1, 1–7.

Santis, B., Debegnach, F., Gregori, E., Russo, S., Marchegiani, F., Moracci, G., Brera, C., 2017. Development of a LC-MS/MS method for the multi-mycotoxin determination in composite cereal-based samples. Toxins 9, 169–181.

Shephard, G.S., 2016. Current status of mycotoxin analysis: a critical review. J. AOAC Int. 99, 842–848.

Smith, M., Madec, S., Coton, E., Hymery, N., 2016. Natural co-occurrence of mycotoxins in foods and feeds and their in vitro combined toxicological effects. Toxins 8 (94), 1–36.

Tang, Z., Liu, X., Su, B., Chen, Q., Cao, H., Yun, Y., Xu, Y., Hammock, B.D., 2020. Ultrasensitive and rapid detection of ochratoxin A in agro-products by a nanobody-mediated FRET-based immunosensor. J. Hazard. Mater. 387, 121678–121685. https://doi.org/10.1016/j.jhazmat.2019.121678.

Tobita, T., Oda, M., Azuma, T., 2004. Segmental flexibility and avidity of IgM in the interaction of polyvalent antigens. Mol. Immunol. 40, 803–811.

Tran, V., Walkenfort, B., Kçnig, M., Salehi, M., Schlücker, S., 2019. Rapid, quantitative, and ultrasensitive point-of-care testing: a portable SERS reader for lateral flow assays in clinical chemistry. Angew. Chem. Int. Ed. 58, 442–446.

Urusov, A.E., Petrakova, A.V., Zherdev, A.V., Dzantiev, B.B., 2016. "Multistage in one touch" design with a universal labelling conjugate for high-sensitive lateral flow immunoassays. Biosens. Bioelectron. 86, 575–579.

Wang, Z., Zong, S., Wu, L., Zhu, D., Cui, Y., 2017. SERS-activated platforms for immunoassay: probes, encoding methods, and applications. Chem. Rev. 117, 7910–7963.

Wang, Y., Lu, M., Tang, D., 2018. Novel photoluminescence enzyme immunoassay based on supramolecular host-guest recognition using L-arginine/ 6-aza-2-thiothymine-stabilized gold nanocluster. Biosens. Bioelectron. 109, 70–74.

Wang, C., Wang, C., Wang, X., Wang, K., Zhu, Y., Rong, Z., Wang, W., Xiao, R., Wang, S., 2019a. Magnetic SERS strip for sensitive and simultaneous detection of respiratory viruses. ACS Appl. Mater. Interface 11, 19495–19505.

Wang, Y., Sun, J., Hou, Y., Zhang, C., Li, D., Li, H., Yang, M., Fan, C., Sun, B., 2019b. A SERS-based lateral flow assay biosensor for quantitative and ultrasensitive detection of interleukin-6 in unprocessed whole blood. Biosens. Bioelectron. 141 (111432), 1–7.

Wu, F., Groopman, J.D., Pestka, J.J., 2014. Public health impacts of foodborne Mycotoxins. Annu. Rev. Food Sci. Technol. 5, 351–372.

Xu, S., Zhang, G., Fang, B., Xiong, Q., Duan, H., Lai, W., 2019. Lateral flow immunoassay based on polydopamine-coated gold nanoparticles for the sensitive detection of zearalenone in maize. ACS Appl. Mater. Interface 11, 31283–31290.

Yang, J., Ren, F.H., Chong, X.Y., Fan, D.L., Chakravarty, S., Wang, Z., Chen, R.T., Wang, A.X., 2014. Guided-mode resonance grating with self-assembled silver nanoparticles for surface-enhanced Raman scattering spectroscopy. Photonics 1, 380–389.

Zhang, D., Huang, L., Liu, B., Ni, H., Sun, L., Su, E., 2018. Quantitative and ultrasensitive detection of multiplex cardiac biomarkers in lateral flow assay with core-shell SERS nanotags. Biosens. Bioelectron. 106, 204–211.

Zhu, C., Zhang, G., Huang, Y., Yang, S., Ren, S., Gao, Z., Chen, A., 2018. Dual-competitive lateral flow aptasensor for detection of aflatoxin B_1 in food and feedstuffs. J. Hazard. Mater. 344, 249–257.